

# Model analysis on thermal UV-cutoff effects on the critical boundary in hot QCD

Jiunn-Wei Chen\*

*Department of Physics and Center for Theoretical Sciences,  
National Taiwan University, Taipei 10617, Taiwan*

Kenji Fukushima†

*Yukawa Institute for Theoretical Physics, Kyoto University, Kyoto 606-8502, Japan*

Hiroaki Kohyama‡

*Institute of Physics, Academia Sinica, Taipei 115, Taiwan and  
Physics Division, National Center for Theoretical Sciences, Hsinchu 300, Taiwan*

Kazuaki Ohnishi§ and Udit Raha¶

*Department of Physics and Center for Theoretical Sciences,  
National Taiwan University, Taipei 10617, Taiwan*

We study the critical boundary on the quark-mass plane associated with the chiral phase transition in QCD at finite temperature. We point out that the critical boundaries obtained from the Lattice QCD simulation and the chiral effective model are significantly different; in the (Polyakov-loop coupled) Nambu–Jona-Lasinio (NJL) model we find that the critical mass is about one order of magnitude smaller than the value reported in the Lattice QCD case. It is known in the Lattice QCD study that the critical mass goes smaller in the continuum limit along the temporal direction. To investigate the temporal UV-cutoff effects quantitatively we consider the (P)NJL model with only finite  $N_\tau$  Matsubara frequencies taken in the summation. We confirm that the critical mass in such a UV-tamed NJL model becomes larger with decreasing  $N_\tau$ , which demonstrates a correct tendency to explain the difference between the Lattice QCD and chiral model results.

PACS numbers: 12.38.Aw, 11.10.Wx, 11.30.Rd, 12.38.Gc

*Introduction* The phase diagram of quark matter as described by Quantum Chromodynamics (QCD) is of great interest in theoretical and experimental physics. Since QCD has been established as the fundamental theory of quarks and gluons, it is our ultimate goal to understand all the phenomena related to the strong interactions from the first principle theory. It is difficult, however, to surpass perturbative calculations due to largeness of the QCD coupling constant in the low-energy regime. One then has to make a choice among non-perturbative techniques such as the Lattice QCD (LQCD) simulation, some effective model descriptions sharing the same global symmetry as QCD, etc. The Lattice QCD (LQCD) is a theoretical framework of quarks and gluons in discretized space-time [1] which is suitable for non-perturbative investigations. The Monte-Carlo simulations in the LQCD have been recently developing to a reliable level not only for hadron spectrums at zero temperature but also for thermal properties in hot QCD matter [2].

Critical phenomena in hot QCD can be studied in the LQCD simulation [3] and it is an important issue

to determine the order of the chiral phase transition as a function of the temperature  $T$  and the quark chemical potential  $\mu$ . In this paper, we study the critical boundary in the chiral phase transition on the quark-mass plane, as represented by the “Columbia plot” [4]. Figure 1 shows a schematic picture of the Columbia plot at  $\mu = 0$  where each point in the parameter space of current quark masses  $\{m_u, m_d, m_s\}$  is marked by its order of the phase transition when  $T$  is raised. Usually one sets  $m_u = m_d (\equiv m_{ud})$  and studies the order of the phase transition on the  $m_{ud}$ - $m_s$  plane. Symmetry arguments show that it should be a first order phase transition in the chiral limit ( $m_{ud} = m_s = 0$ ) [5], while for intermediate quark masses at which both chiral and center symmetries are badly broken, only a smooth crossover is possible. This defines the second-order critical phase boundary that separates the first-order and crossover regions.

The “phys. point” in Fig. 1 designates the “real world” with physical current quark masses ( $m_{ud} = 5.5$  MeV and  $m_s = 135.7$  MeV in a model study), whose location should crucially decide the order of the phase transition at  $\mu = 0$ . More importantly, the distance between the second-order critical boundary and the physical point on the Columbia plot gives a rough measure of how far the QCD critical point is separated from the  $\mu = 0$  situation. Roughly speaking, the farther the physical point is located away from the critical boundary, the larger  $\mu$  is necessary to make the critical surface hit on the physical

---

\*Electronic address: jwc@phys.ntu.edu.tw

†Electronic address: fuku@yukawa.kyoto-u.ac.jp

‡Electronic address: kohyama@phys.sinica.edu.tw

§Electronic address: kohnishi@phys.ntu.edu.tw; Present affiliation: GOGA, Inc., Tokyo.

¶Electronic address: udit.raha@unibas.ch

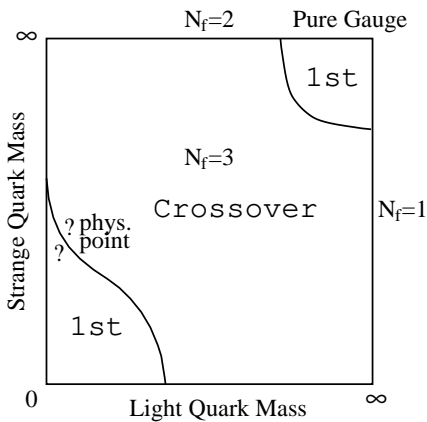


FIG. 1: Columbia plot at finite  $T$  and  $\mu = 0$ .

point.

The critical boundary can also be analyzed by means of the LQCD simulation since the Columbia plot is drawn at zero baryon density, where the Binder cumulant is a useful quantity to identify the order of the phase transition [6, 7, 8]. To draw the Columbia plot we can use the three-flavor Nambu–Jona-Lasinio (NJL) model [9] which is a model of quarks with the effective Lagrangian so constructed to have the same global symmetry as QCD [10, 11]. (For other chiral model studies see [12, 13].) Gauge symmetry is, however, absent due to the absence of gluons in the model. It is a crucial aspect in the NJL model to incorporate chiral symmetry as an important ingredient in understanding the properties of light hadrons. Further, the model can successfully describe the spontaneous breaking of chiral symmetry at in the QCD vacuum and its restoration at high temperature and/or density. The three-flavor NJL model gives a first order phase transition in the chiral limit by virtue of the  $U_A(1)$  symmetry breaking term [5], while, at intermediate quark mass, the chiral restoration results in a crossover due to explicit chiral symmetry breaking by finite quark mass as long as  $\mu \simeq 0$ . Thus, the NJL model should be able to reproduce the expected structure of the Columbia plot (i.e. critical boundary in the left-bottom corner in Fig. 1), which can be compared with the LQCD results.

Although the NJL model successfully describes the qualitative feature of the chiral phase transition, there remains a significant difference between the critical boundaries from the NJL model and the LQCD simulations. In fact, the value of the critical quark mass is about one order of magnitude different, which is crucial in the QCD critical point search. One may have seen a scatter plot of the critical point locations from the LQCD attempts as well as the chiral model approaches as shown in [14]. However, there is a huge discrepancy in the critical mass boundary already at zero baryon density depending on the adopted methods, and then, how can one trust any of them at finite density? Let us pick some concrete num-

bers up. We define the critical quark mass  $m_c$  as a point where the  $m_{ud} = m_s$  symmetric line intersects with the critical boundary. Then,  $m_c$  is around 14 MeV in the LQCD simulation [6] but it is only 1.1 MeV from the NJL model.

In the LQCD studies [7, 8], it was argued that the first-order region drastically shrinks by removal of the discretization errors. In [8], for example, the authors used the Symanzik improved gauge and stout improved fermionic action and concluded that the critical mass goes below 7% (and 12%) of the physical quark mass on the  $N_\tau = 4$  (and  $N_\tau = 6$  respectively) lattice. The conclusion in [7] is consistent with this qualitatively though the quantitative change is not such drastic. Because the number of spatial points is large enough (16, 24, etc) in the LQCD simulations, smallness of  $N_\tau$  in the temporal direction is crucial. In other words, the temporal UV cutoff  $\pi N_\tau T$  has drastic effects on the critical mass boundary even at zero density (and hence on the QCD critical point at finite density as well, which is beyond our current scope in this paper).

Here, we shall examine the chiral critical boundary by imposing a finite UV cutoff in the temporal (thermal) direction in the NJL model to mimic the LQCD situation. In this way, we can give a quantitative prediction about how much the critical boundary moves by the finite  $N_\tau$  effects. In terms of Fourier transformed variables the summation over finite- $N_\tau$  temporal sites amounts to the Matsubara summation over finite- $N_\tau$  frequencies. Hereafter, throughout this paper, we will drop the subscript and simply write as  $N$  for notational simplicity. In what follows, we present a brief description of this modified NJL model and discuss the machinery of how to deal with finite  $N$  in this model treatment. Later, we shall also present some results using the Polyakov-loop coupled NJL (PNJL) model [9, 15, 16, 17, 18], for the PNJL model is a much better description of QCD thermodynamics near the critical temperature.

*Modified NJL model* The three-flavor NJL model Lagrangian is,

$$\mathcal{L}_{\text{NJL}} = \bar{q}(i\partial - \hat{m})q + \mathcal{L}_4 + \mathcal{L}_6, \quad (1)$$

$$\mathcal{L}_4 = \frac{g_S}{2} \sum_{a=0}^8 \left[ (\bar{q}\lambda_a q)^2 + (\bar{q}i\gamma_5\lambda_a q)^2 \right], \quad (2)$$

$$\mathcal{L}_6 = -g_D [\det \bar{q}_i(1 - \gamma_5)q_j + \text{h.c.}]. \quad (3)$$

The current quark mass matrix  $\hat{m}$  in the kinetic term takes the diagonal form  $\hat{m} = (m_u, m_d, m_s)$ , and we set  $m_u = m_d$  ( $\equiv m_{ud}$ ). In the above  $\mathcal{L}_4$  expresses the four-fermion contact interaction with the coupling constant  $g_S$ , where  $\lambda_a$  is the Gell-Mann matrix in flavor space, and  $\mathcal{L}_6$  is the Kobayashi-Maskawa-'t Hooft interaction [19, 20, 21] with the coupling strength  $g_D$ . The determinant runs over the flavor indices, which leads to six-fermion interaction terms in the three-flavor case. This interaction explicitly breaks the  $U_A(1)$  symmetry, whose microscopic origin comes from instantons [21].

We should solve the gap equations which we can get by differentiating the thermodynamic potential  $\Omega$  with respect to the constituent quark masses;

$$\frac{\partial \Omega}{\partial m_u^*} = 0, \quad \frac{\partial \Omega}{\partial m_s^*} = 0. \quad (4)$$

Here  $m_u^*$  and  $m_s^*$  are the constituent masses for  $u$  and  $s$  quarks. The thermodynamic potential is defined by  $\Omega = -\ln Z/(\beta V)$ , with the partition function  $Z$ , the inverse temperature  $\beta = 1/T$ , and the volume of the system  $V$ .

In the mean-field approximation for the NJL Lagrangian (1) we obtain the following gap equations,

$$\begin{aligned} m_u^* &= m_u + 2i g_S N_c \text{tr} S^u - 2g_D N_c^2 (\text{tr} S^u)(\text{tr} S^s), \\ m_s^* &= m_s + 2i g_S N_c \text{tr} S^s - 2g_D N_c^2 (\text{tr} S^u)^2. \end{aligned} \quad (5)$$

Here  $N_c = 3$  is the number of colors and  $\text{tr} S^i$  is the chiral condensate given explicitly by

$$i \text{tr} S^i = 4m_i^* \int \frac{d^3 p}{(2\pi)^3} (iT) \sum_{n=-\infty}^{\infty} \frac{i}{(i\omega_n)^2 - E_i^2}, \quad (6)$$

where the Matsubara frequency is  $\omega_n = (2n+1)\pi T$  and the quasi-particle energy is  $E_i = \sqrt{\mathbf{p}^2 + m_i^{*2}}$ . A detailed derivation of the gap equations is clearly given in [10, 11].

To study the effect of the finite cutoff in the temporal direction on the critical boundary, we then perform the following modification in the Matsubara frequency sum;

$$\sum_{n=-\infty}^{\infty} \rightarrow \sum_{n=-N+1}^N. \quad (7)$$

We shall reveal the critical boundary in the  $m_{ud}$ - $m_s$  plane for various values of  $N$ . To this end, we adjust the model parameters to fit the physical quantities for a given  $N$  (each parameter set representing a modified NJL model with a different temporal cutoff). This is reminiscent of the familiar Wilsonian renormalization group (RG) flow. After the high frequency modes are integrated out, in principle, the coefficients of the operators run on the RG flow. Here we remark that we neglect interaction operators in other channels than those in Eqs. (1)-(3) since their effects are small in the mean-field calculations performed below (see e.g., [10] and refs. therein).

The following are the model parameters in the three-flavor NJL model;

$$\begin{array}{ll} \text{current quark masses} & m_{ud}, m_s, \\ \text{three-momentum cutoff} & \Lambda, \\ \text{four-point coupling constant} & g_S, \\ \text{six-point coupling constant} & g_D. \end{array}$$

As for the light current quark masses, we fix  $m_{ud} = 5.5$  MeV following [11], which gives isospin symmetric results and thus  $m_u^* = m_d^*$ . The remaining parameters are determined by a fit to the four physical quantities: the pion

$N$	$m_s$ (MeV)	$\Lambda$ (MeV)	$g_S \Lambda^2$	$g_D \Lambda^5$
15	134.7	631.4	4.16	12.51
20	135.0	631.4	4.02	11.56
50	135.3	631.4	3.82	10.14
100	135.4	631.4	3.75	9.69
$\infty$	135.7	631.4	3.67	9.29

TABLE I: Fitted parameters for various values of  $N$ .

mass  $m_\pi$ , the pion decay constant  $f_\pi$ , the kaon mass  $m_K$ , and the  $\eta'$  mass  $m_{\eta'}$ , whose empirical values are

$$\begin{aligned} m_\pi &= 138 \text{ MeV}, & f_\pi &= 93 \text{ MeV}, \\ m_K &= 495.7 \text{ MeV}, & m_{\eta'} &= 958 \text{ MeV}. \end{aligned} \quad (8)$$

*Numerical results* The limit of  $N = \infty$  invariably corresponds to the standard framework of the NJL model and we then use the same parameter set fixed in [11]. For finite  $N$ , we have picked up a temperature  $T = 50$  MeV at which we have carried out our fitting procedure. This choice is just because of technical convenience. Besides, calculations at  $T = 50$  MeV should be sufficiently close to those at zero temperature since the constituent quark mass is then several times larger than the temperature. The fitted parameters in this way for  $N = 15, 20, 50, 100$  at  $T = 50$  MeV are displayed in Tab. I.

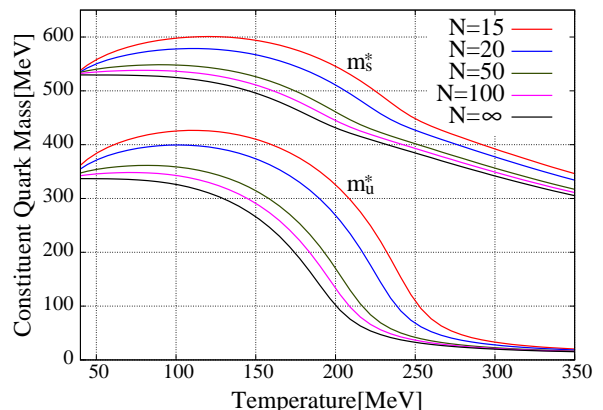


FIG. 2: Constituent quark masses  $m_u^*$  (lower) and  $m_s^*$  (upper) as a function of  $T$  for various values of  $N$ .

As seen from the table, the couplings  $g_S$  and  $g_D$  become larger with decreasing  $N$ . If we fixed the coupling constants, the effect of smaller  $N$  would be to reduce the constituent quark masses. Therefore, to keep  $m_i^*$  unchanged, we need larger  $g_S$  and  $g_D$  to compensate for this reduction (see Eq. (5)). Note that, as expected, the whole behavior of  $m_u^*$ ,  $m_s^*$  as a function of  $T$  monotonically approach the standard (i.e.  $N = \infty$ ) case with increasing  $N$ . In Fig. 2, we only show the numerical results above  $T = 40$  MeV because the small- $T$  region is badly affected by finite  $N$  and the calculations are no longer reliable there. We can understand this intuitively;  $1/T$  is the extent along the imaginary-time (thermal) direction

and thus, the extent becomes longer as  $T$  goes smaller. Hence, at lower  $T$ , reliable estimates need more  $N$ . This means, fixing the value of  $N$ , the choice of the small- $T$  regions would automatically lead to unphysical results.

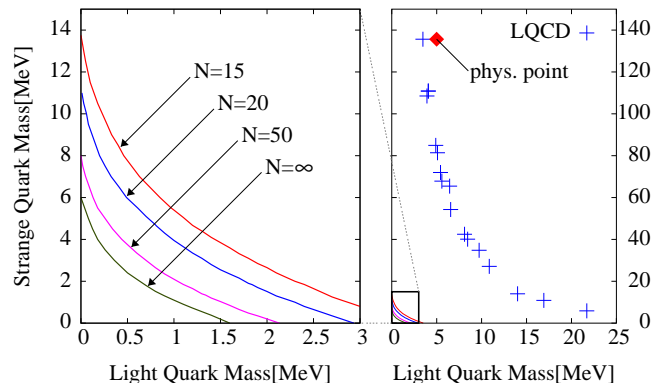


FIG. 3: Critical boundaries on the  $m_{ud}-m_s$  plane in the NJL model (left panel) as compared with the LQCD results with  $N_\tau = 4$  (right panel).

In Fig. 3, we display the result for the critical boundary in our modified NJL model with the finite Matsubara frequency summations:  $N = 15, 20, 50, \infty$ , along with the results from the LQCD simulation with  $N_\tau = 4$  [6] for comparison. We find that the first-order region widens as  $N$  decreases. This observation qualitatively agrees with the arguments in the LQCD simulations that the first-order region tends to get bigger than its genuine size due to the finite UV-cutoff effects. Quantitatively, however, the critical boundaries still look far from the LQCD results at  $N_\tau = 4$ . We comment that not only the temporal UV-cutoff but also the spatial (three-momentum) cutoff leads to similar alteration in the critical boundary i.e., we have found that lowering  $\Lambda$  also pushes the critical mass up, though such effects are only minor.

*The PNJL model extension* It is also worth studying the critical boundary using the PNJL model [9, 15, 16, 17, 18]. This is because, in view of the results in [22, 23], the location of the critical point is significantly moved toward higher  $T$  by the inclusion of the Polyakov loop which suppresses unphysical quark excitations. Furthermore, the PNJL model is quite successful to reproduce the LQCD observables for QCD thermodynamics such as the quark number susceptibility, the interaction measure, the sound velocity, etc. Because the PNJL model nicely grasps the essential nature of the QCD phase transitions, it would be rather mysterious if only the critical boundary on the  $m_{ud}-m_s$  shows a huge discrepancy.

The model is defined by the following Lagrangian [15,

16],

$$\mathcal{L}_{\text{PNJL}} = \mathcal{L}_0 + \mathcal{L}_4 + \mathcal{L}_6 + \mathcal{U}(\Phi, \Phi^*, T), \quad (9)$$

$$\mathcal{L}_0 = \bar{q}(i\cancel{\partial} - i\gamma_4 A_4 - \hat{m})q, \quad (10)$$

$$\mathcal{U}(\Phi, \Phi^*, T) = -bT\{54e^{-a/T}\Phi\Phi^* + \ln[1 - 6\Phi\Phi^* + 4(\Phi^3 + \Phi^{*3}) - 3(\Phi\Phi^*)^2]\}, \quad (11)$$

where  $\mathcal{U}$  is the effective potential in terms of the Polyakov loop. Here  $\Phi$  and  $\Phi^*$  are the traced Polyakov loop and the anti-Polyakov loop which are order parameters for deconfinement. They are defined by  $\Phi = (1/N_c)\text{tr}L$ ,  $\Phi^* = (1/N_c)\text{tr}L^\dagger$  with  $L = \mathcal{P}\exp[i\int_0^\beta d\tau A_4]$ . We set the parameters  $a$  and  $b$  as  $a = 664$  MeV,  $b \cdot \Lambda^{-3} = 0.03$  following [9].

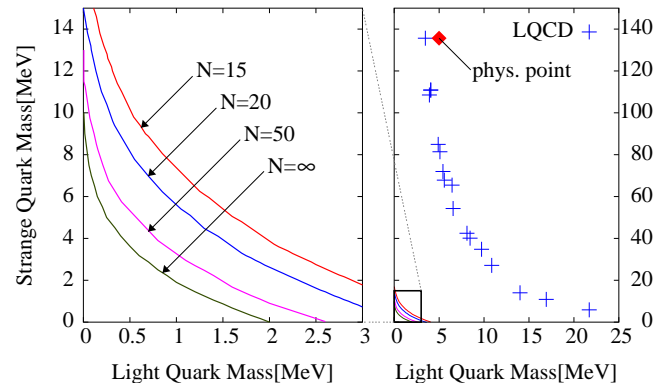


FIG. 4: Critical boundaries on the  $m_{ud}-m_s$  plane in the PNJL model (left panel) as compared with the LQCD results with  $N_\tau = 4$  (right panel).

Because the Polyakov-loop part is relevant only at finite  $T$  (as high as comparable with  $T_c$ ), we can simply employ the same parameter sets, as fixed previously in the NJL model case with finite  $N$  (see Tab. I). Then, we show the results for the critical boundary determined by the same procedure in Fig. 4. Here again, we see expanding behavior of the first-order region with decreasing  $N$ . Although the PNJL results are quantitatively different from the NJL ones, the qualitative tendency is the same and, besides, the difference is not really substantial. The fact that the PNJL model results are such close to the NJL ones is in fact non-trivial. The Polyakov loop generally governs the thermal excitation of quarks near  $T_c$  and particularly unphysical quarks below  $T_c$  are prohibited by small  $\Phi$  and  $\Phi^*$ . This leads to the consequence that the critical point temperature is lifted up to twice as high. From the comparison between Figs. 3 and 4, gives us confidence that the smallness of the first-order region is *not* simply an NJL-model artifact with unphysical quark excitations.

*Concluding remarks* Our model analysis yields intriguing results that the critical masses become larger with truncation in the Matsubara frequency summation.

This effect is not large enough to give a full account for the quantitative difference in the critical boundaries between the LQCD and NJL model studies. Nevertheless, it raises an interesting possibility that the critical masses in the LQCD simulation become smaller if the LQCD simulation accommodates larger  $N_\tau$ . This is an important message since the LQCD simulation at  $N_\tau = 4, 6$ , and even 8 may have a potential danger that the LQCD simulation overestimates the strength of the first-order phase transition, and thus the critical point emerges at small density due to lattice artifacts.

An interesting extension of our study is to determine the chiral phase transition boundary on the plane with  $T$  and the baryon (quark) chemical potential  $\mu$ . It is a common folklore that the QCD critical point should appear at some  $T_E$  and  $\mu_E$ . However, it is highly non-trivial to determine the order of the phase transition at non-zero  $\mu$ . Recent LQCD simulations at small  $\mu$  (i.e. expansion as a power of  $\mu/T$ ) disfavor the existence of the critical point

in the QCD phase diagram [6, 7]. There have been theoretical efforts to understand this LQCD finding in the context of the chiral effective model approaches [24, 25]. However, the errors of the LQCD simulations grow bigger at higher  $\mu$  and, to be worse, the (P)NJL-model analyses can be trusted only at a qualitative level so far once  $\mu$  gets large. It is still inconclusive, therefore, whether the critical point actually exists or not. Our model analysis shows that increasing  $N_\tau$  leads to smaller critical quark masses. This result might indicate to further minify the possibility for finding the QCD critical point using the LQCD simulation unless the discretization errors are under good theoretical control.

JWC, KO and UR are supported by the NSC and NCTS of Taiwan. KF is supported in part by Japanese MEXT grant No. 20740134 and the Yukawa International Program for Quark Hadron Sciences. UR also thanks INT, Seattle for the kind hospitality during the course of this work.

- 
- [1] K. G. Wilson, Phys. Rev. D **10**, 2445 (1974).  
 [2] For a recent review, see; O. Philipsen, Prog. Theor. Phys. Suppl. **174**, 206 (2008) [arXiv:0808.0672 [hep-ph]].  
 [3] S. Ejiri *et al.*, arXiv:0909.5122 [hep-lat].  
 [4] F. R. Brown *et al.*, Phys. Rev. Lett. **65**, 2491 (1990).  
 [5] R. D. Pisarski and F. Wilczek, Phys. Rev. D **29**, 338 (1984).  
 [6] P. de Forcrand and O. Philipsen, JHEP **0701**, 077 (2007) [arXiv:hep-lat/0607017].  
 [7] P. de Forcrand, S. Kim and O. Philipsen, PoS **LAT2007**, 178 (2007) [arXiv:0711.0262 [hep-lat]]; P. de Forcrand and O. Philipsen, JHEP **0811**, 012 (2008) [arXiv:0808.1096 [hep-lat]].  
 [8] G. Endrodi, Z. Fodor, S. D. Katz and K. K. Szabo, PoS **LAT2007**, 182 (2007) [arXiv:0710.0998 [hep-lat]].  
 [9] K. Fukushima, Phys. Rev. D **77**, 114028 (2008) [Erratum-ibid. D **78**, 039902 (2008)] [arXiv:0803.3318 [hep-ph]].  
 [10] S. P. Klevansky, Rev. Mod. Phys. **64**, 649 (1992).  
 [11] T. Hatsuda and T. Kunihiro, Phys. Rept. **247**, 221 (1994) [arXiv:hep-ph/9401310].  
 [12] P. Kovacs and Z. Szep, Phys. Rev. D **75**, 025015 (2007) [arXiv:hep-ph/0611208].  
 [13] B. J. Schaefer and M. Wagner, Phys. Rev. D **79**, 014018 (2009) [arXiv:0808.1491 [hep-ph]].  
 [14] M. A. Stephanov, Prog. Theor. Phys. Suppl. **153**, 139 (2004) [Int. J. Mod. Phys. A **20**, 4387 (2005)] [arXiv:hep-ph/0402115].  
 [15] K. Fukushima, Phys. Lett. B **591**, 277 (2004) [arXiv:hep-ph/0310121].  
 [16] C. Ratti, M. A. Thaler and W. Weise, Phys. Rev. D **73**, 014019 (2006) [arXiv:hep-ph/0506234].  
 [17] W. j. Fu, Z. Zhang and Y. x. Liu, Phys. Rev. D **77**, 014006 (2008) [arXiv:0711.0154 [hep-ph]].  
 [18] M. Ciminale, R. Gatto, N. D. Ippolito, G. Nardulli and M. Ruggieri, Phys. Rev. D **77**, 054023 (2008) [arXiv:0711.3397 [hep-ph]].  
 [19] M. Kobayashi and T. Maskawa, Prog. Theor. Phys. **44**, 1422 (1970).  
 [20] M. Kobayashi, H. Kondo and T. Maskawa, Prog. Theor. Phys. **45**, 1955 (1971).  
 [21] G. 't Hooft, Phys. Rev. Lett. **37**, 8 (1976).  
 [22] S. Roessner, C. Ratti and W. Weise, Phys. Rev. D **75**, 034007 (2007) [arXiv:hep-ph/0609281].  
 [23] D. Gomez Dumm, D. B. Blaschke, A. G. Grunfeld and N. N. Scoccola, Phys. Rev. D **78**, 114021 (2008) [arXiv:0807.1660 [hep-ph]].  
 [24] K. Fukushima, Phys. Rev. D **78**, 114019 (2008) [arXiv:0809.3080 [hep-ph]].  
 [25] J. W. Chen, K. Fukushima, H. Kohyama, K. Ohnishi and U. Raha, Phys. Rev. D **80**, 054012 (2009) [arXiv:0901.2407 [hep-ph]].